Journal of Renewable Materials

Tech Science Press

https://doi.org/10.32604/jrm.2026.02026-0012

ARTICLE

Engineering Microporous Bamboo-Derived Carbons via Alkaline Activation for Formaldehyde Adsorption in Building Environments

Ju He[1,#], Peiwen Zhao[2,#], Dongyang Han[3], Kexin Lv[2], Jiuping Rao[3,*], Xinqiang Ye[4], Guodong Ruan[4], Fei Guo[3], Mizi Fan[3,*] and Weigang Zhao[3,*]

[1]College of Landscape Architecture, Fujian Agriculture and Forestry University, 63 Xiyuangong Road, Fuzhou, China
[2]College of Transportation and Civil Engineering, Fujian Agriculture and Forestry University, Fuzhou, China
[3]College of Material Engineering, Fujian Agriculture and Forestry University, Fuzhou, China
[4]Fujian Yongan Forestry (Group) Co., Ltd., No. 819 Yanjiang East Rd., Yong'an, China

*Corresponding Authors: Jiuping Rao. Email: rjustin@fafu.edu.cn; Mizi Fan. Email: mizi.fan@brunel.ac.uk; Weigang Zhao. Email: weigang-zhao@fafu.edu.cn

[#]These authors contributed equally to this work

Received: 27 January 2026; Accepted: 26 March 2026; Published: 24 April 2026

ABSTRACT: This study presents a systematic evaluation of bamboo-derived activated carbons (ACs) prepared using three alkaline activating agents-KOH, $KHCO_3$, and K_2CO_3-for efficient formaldehyde adsorption. The pore structures of the resulting ACs were modulated by varying the alkali-to-carbon (A/C) ratio from 1:1 to 4:1, and the effects on microstructure and adsorption performance were thoroughly investigated. Among all samples, AC-MB@KOH(3) demonstrated superior performance, featuring a high specific surface area of 2141.77 m^2/g and a removal efficiency of 90%, attributed to its rich microporous texture and well-developed hierarchical porosity. Comparative analysis revealed that the activation strength and decomposition behavior of different alkaline agents critically influenced pore formation dynamics and gas diffusion pathways. Correlation analysis indicated a strong linear relationship between formaldehyde removal efficiency and micropore volume (R^2 = 0.87), emphasizing the pivotal role of micropores in gas molecule capture. These findings underscore the advantages of strong alkaline activation and offer a theoretical foundation for designing high-efficiency, biomass-derived porous adsorbents for indoor air purification applications.

KEYWORDS: Bamboo-based activated carbon; alkaline activation; formaldehyde removal; microporous structure; indoor air purification

1 Introduction

In modern architectural design and building engineering, indoor air quality (IAQ) has become a central issue that directly affects human health, comfort, and well-being [1–5]. With the advent of energy-efficient buildings and airtight envelopes, indoor environments are increasingly prone to the accumulation of volatile organic compounds (VOCs), which are released from construction materials, furniture, decorative finishes, and household chemicals [6,7]. Among the various VOCs, formaldehyde (HCHO) is one of the most ubiquitous and hazardous contaminants due to its persistent emission characteristics and adverse health effects [8–10]. It is a potent irritant, a respiratory sensitizer, and a Group I carcinogen as classified by the International Agency for Research on Cancer (IARC) [11]. Given its widespread occurrence in interior spaces-from flooring adhesives and artificial board to paints and textiles-formaldehyde is a representative

indoor VOC widely used to evaluate the adsorption performance of porous materials in building-related applications [12–15].

To mitigate formaldehyde pollution in built environments, various removal techniques have been developed, such as catalytic oxidation, chemical absorption, photocatalysis, and plant-based biological filtration [16–19]. However, these methods often suffer from high cost, poor scalability, sensitivity to environmental conditions (e.g., humidity, temperature), and limited removal efficiency under low pollutant concentrations [20]. In contrast, physical adsorption using porous carbon materials has garnered considerable attention as a promising route due to its simplicity, environmental friendliness, and broad adaptability to indoor applications. In particular, adsorption-based modules can be easily integrated into building ventilation systems, wall or floor panels, or portable air purifiers without the need for complex control systems [21–23].

Activated carbon (AC) remains one of the most effective adsorbents for VOC removal owing to its large specific surface area, high thermal stability, and tunable pore structure [24,25]. However, traditional ACs-especially those derived from fossil-based or industrial feedstocks-are often limited by their low selectivity for polar, small-sized molecules such as formaldehyde. This is primarily attributed to the insufficient proportion of ultra-micropores (pore width < 0.7 nm) and lack of surface polar functional groups, which restrict the interaction between the adsorbent and the target molecule [26–28]. Recent efforts to enhance the adsorption performance of ACs have focused on two major approaches: (I) introducing heteroatoms such as N or O through doping or post-treatment, which enhances surface polarity and chemical affinity; and (II) optimizing pore architecture, especially the hierarchical arrangement of micropores and mesopores, to improve both uptake capacity and mass transport dynamics [29–32]. Despite these developments, a unified understanding of how pore structure characteristics (micro- and meso- pores) correlate with adsorption performance remains an open research challenge.

Alkaline chemical activation has emerged as a widely adopted method for tailoring the pore structure of carbon materials due to its controllability, scalability, and cost-effectiveness [33–36]. Among alkaline agents, potassium-based activators such as KOH, $KHCO_3$, and K_2CO_3 are frequently used. These activators differ significantly in their thermal decomposition pathways, gas evolution behavior, and reactivity with carbon precursors. KOH, a strong base, induces aggressive carbon etching and promotes *in-situ* formation of potassium species together with the evolution of gaseous products such as H_2, CO, and CO_2 during high-temperature activation, resulting in explosive pore expansion and the development of an interconnected micro-/mesoporous framework [37,38]. In contrast, $KHCO_3$ and K_2CO_3 are milder activators that undergo gradual decomposition and generate fewer pore-forming species, often resulting in lower surface areas and narrower pore size distributions [39–41]. Importantly, the activation strength, pore development kinetics, and microstructural outcomes are highly dependent on the alkali-to-carbon ratio, activation temperature, and raw material characteristics [42]. Therefore, a comparative mechanistic investigation of these alkaline systems is essential for the rational design of high-performance formaldehyde adsorbents.

Recent studies have demonstrated that wood- and bamboo-based materials can be engineered into multifunctional systems for energy storage, environmental remediation, flexible electronics, and gas purification through multiscale structural regulation and chemical modification [43,44]. For instance, recent reviews have highlighted that the intrinsic hierarchical structure of bamboo provides a versatile platform for developing advanced functional materials with tunable physical and chemical properties. In addition, bio-inspired bamboo-based porous structures have shown promising performance in air purification and pollutant capture applications [45]. Among the various forms of biomass-derived functional materials, porous carbons prepared from renewable biomass have attracted particular interest due to their tunable pore structures, high surface areas, and chemical stability, making them highly suitable for adsorption-related applications.

The development of efficient biomass-derived porous carbons therefore represents an important strategy for converting abundant natural resources into value-added functional materials. Meanwhile, the selection of sustainable carbon precursors is of paramount importance in the context of green building materials and circular economy goals. Bamboo is a highly promising renewable biomass resource that has attracted growing interest due to its rapid growth cycle, widespread availability, and excellent physicochemical properties [45–47]. Rich in cellulose, hemicellulose, and lignin, bamboo offers a robust fibrous matrix and high carbon yield, which facilitates the formation of stable porous carbon structures upon pyrolysis [48,49]. Additionally, the hierarchical vascular structure of bamboo enables the generation of multi-level pores that are advantageous for gas diffusion and adsorption [50,51]. From a sustainability perspective, bamboo-derived carbons contribute to both carbon neutrality and low-emission construction, aligning with global trends in green infrastructure, healthy buildings, and net-zero architecture.

Moso bamboo is one of the most widely distributed bamboo species in China and is frequently used as a precursor for biomass-derived carbon materials due to its high lignocellulosic content and stable structural characteristics. In this study, we develop a series of bamboo-based activated carbons (BACs) via high-temperature pyrolysis and alkaline activation using KOH, KHCO3, and K_2CO_3 as representative activators. By systematically tuning the alkali-to-carbon ratio and comparing the resulting textural properties, we investigate the interplay between activation chemistry, pore architecture, and formaldehyde adsorption performance. N_2 physisorption and SEM analysis are conducted to uncover structure–performance correlations. Furthermore, formaldehyde adsorption is assessed under ambient conditions to simulate indoor environments. Through this comparative approach, we aim to (I) elucidate the activation mechanisms of different alkaline agents, (II) optimize pore structure engineering for VOC removal, and (III) promote the high-value utilization of bamboo biomass in sustainable building materials and indoor air quality enhancement.

2 Experimental Section

2.1 Materials

Bamboo raw materials (Moso bamboo, *Phyllostachys edulis*) were sourced from Fujian Province, China. The bamboo used in this study was approximately 3 years old, which is commonly used for biomass carbon preparation due to its stable lignocellulosic composition. Potassium hydroxide (KOH), potassium carbonate (K_2CO_3), potassium bicarbonate ($KHCO_3$), and hydrochloric acid (HCl, 36%–38%) were of analytical grade and obtained from Tianjin Zhiyuan Chemical Reagent Co., Ltd. All reagents were used without further purification.

2.2 Preparation of Bamboo-Based Activated Carbons

Fresh bamboo segments were washed thoroughly and oven-dried at 103°C until constant weight. The dried bamboo was then ground and sieved through a 200-mesh screen to obtain uniform bamboo powder as the carbon precursor. A total of 3.0 g of the pre-carbonized bamboo powder (denoted as C-MB) was carbonized at 500°C for 1 h under nitrogen atmosphere (flow rate: ~500 mL/min) using a muffle furnace to obtain the base carbon material. The resulting C-MB was mixed with KOH, $KHCO_3$, or K_2CO_3 at different mass ratios (1:1, 1:2, 1:3, and 1:4), placed in a nickel crucible, and activated in a tubular furnace by heating to 800°C at 5°C/min under N_2. The sample was held at 800°C for 2 h and allowed to cool naturally. After activation, the products were washed with 1 mol/L HCl and then rinsed with deionized water until the pH stabilized. To ensure high purity, Soxhlet extraction with deionized water was performed for 48 h. Finally, the samples were dried at 105°C for 12 h. The resulting activated carbon samples were denoted as AC-MB@X(Y), where X represents the activator (KOH, $KHCO_3$, or K_2CO_3) and Y indicates the mass ratio (Fig. 1).

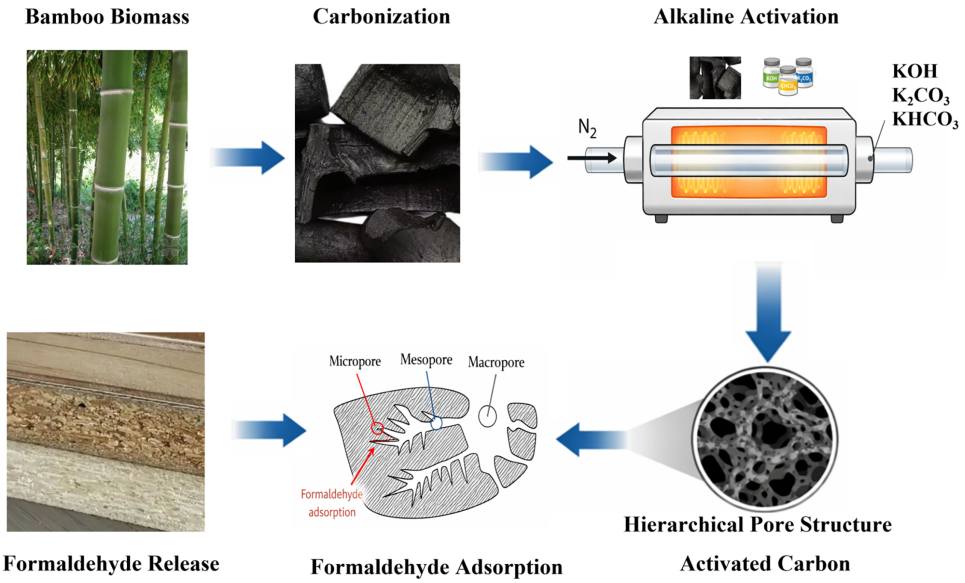

Figure 1: Schematic illustration of the preparation of bamboo-based activated carbons using different alkaline activators.

2.3 Characterization and Formaldehyde Adsorption Test

The textural properties of the samples were analyzed using N_2 adsorption-desorption isotherms at 77 K with a BET surface area analyzer (ASAP 2020, Micromeritics, USA). Specific surface area (S_{BET}) was determined by the Brunauer-Emmett-Teller (BET) method, and pore volume and distribution were calculated via the Density Functional Theory (DFT) model, yielding total pore volume ($V_{0.99}$), micropore volume (V_{micro}), and mesopore volume (V_{meso}). The morphology and microstructure of the samples were observed using scanning electron microscopy (SEM, Regulus 3400, Hitachi, Japan), while the elemental composition and distribution were obtained via energy-dispersive X-ray spectroscopy (EDS).

The formaldehyde adsorption performance was evaluated using a sealed-chamber method (Fig. 2). Formaldehyde vapor was generated by adding a measured volume of formaldehyde solution (37 wt%) to a Petri dish inside an 8.5 L airtight chamber. After equilibration, a pre-weighed adsorbent was introduced into the chamber through a sample release device, initiating the adsorption process. It should be noted that the present adsorption experiments were conducted using a sealed-chamber removal test designed to simulate indoor air purification conditions. Therefore, the obtained results mainly reflect removal efficiency under dilute gas-phase conditions rather than equilibrium adsorption isotherms.

Formaldehyde concentration was continuously monitored using a real-time detector until equilibrium was reached. The adsorption capacity and removal efficiency were calculated using the following equations:

$$q_e = (C_0 - C_t)V/m.$$

$$R = \frac{C_0 - C_t}{C_0} \times 100\%.$$

where:

q is the adsorption capacity (mg/g),

R is the formaldehyde removal efficiency (%),

C_0 and C_t are the initial and final formaldehyde concentrations (mg/m^3),

V is the chamber volume (m^3),

m is the mass of the adsorbent (g).

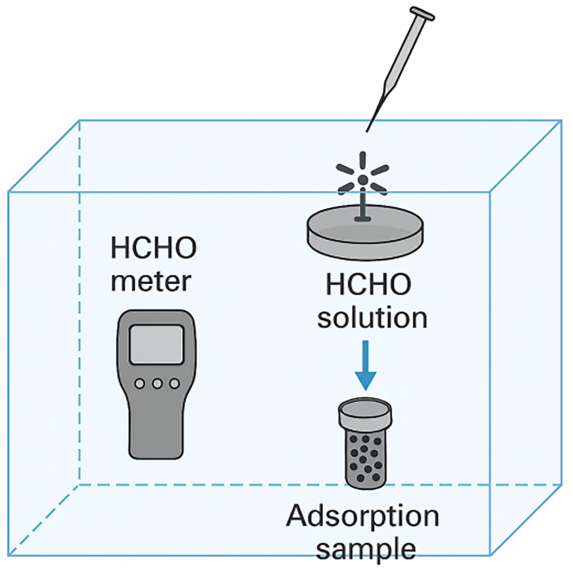

Figure 2: Schematic diagram of the formaldehyde adsorption device.

3 Results and Discussion

3.1 Pore Structure and Formaldehyde Adsorption Performance

3.1.1 KOH-Activated Bamboo-Based Carbon

To investigate the influence of KOH activation on the pore structure and formaldehyde adsorption performance of bamboo-derived carbon, a series of samples were prepared using different alkali-to-carbon (A/C) ratios and tested in sealed-chamber adsorption experiments. As illustrated in Fig. 3, the formaldehyde adsorption capacity steadily increased with rising KOH dosage. Among the samples, AC-MB@KOH(3), synthesized at an A/C ratio of 3:1, exhibited the highest adsorption capacity of 0.34 mg/g and a formaldehyde removal efficiency of 90%. However, when the A/C ratio was further increased to 4:1, the adsorption performance slightly declined, indicating that excessive KOH may induce structural damage, such as pore wall collapse or excessive pore widening. As shown in Table 1, when the A/C ratio increases beyond the optimal value, the micropore volume (V_{micro}) no longer increases proportionally with S_{BET}, indicating that excessive activation may enlarge or partially collapse microporous structures. These structural defects could decrease the proportion of effective micropores, thereby reducing the material's selective adsorption ability for small gas molecules. It should be noted that in the present study, adsorption tests were conducted under low-concentration gas-phase conditions designed to simulate indoor air environments. Under such dilute conditions, the measured adsorption capacity is naturally lower, while removal efficiency becomes a more relevant performance indicator.

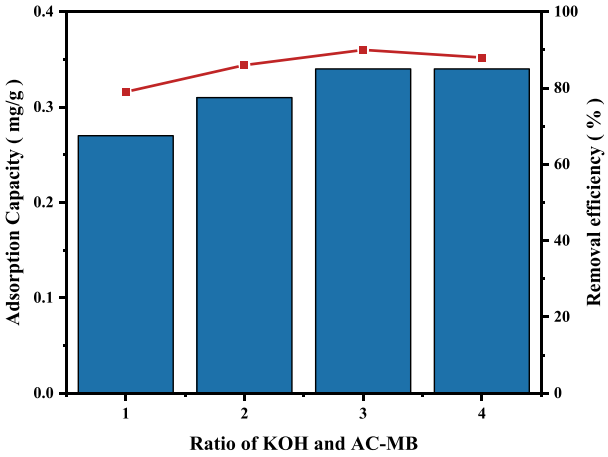

Figure 3: Formaldehyde adsorption performance of KOH-activated bamboo-derived carbon with different alkali-to-carbon ratios.

Table 1: Pore structure parameters of KOH-activated bamboo-derived carbon.

Sample	S_{BET} (m^2/g)	$V_{0.99}$ (cm^3/g)	V_{micro} (cm^3/g)	V_{meso} (cm^3/g)
AC-MB@KOH(1)	1526.75	0.67	0.57	0.10
AC-MB@KOH(2)	1969.51	1.10	0.70	0.40
AC-MB@KOH(3)	2141.77	1.26	0.76	0.50
AC-MB@KOH(4)	2576.16	1.64	0.93	0.71

To elucidate the relationship between pore structure and adsorption behavior, nitrogen adsorption–desorption isotherms were obtained and are presented in Fig. 4a. All samples exhibited type-I isotherms (IUPAC classification), characteristic of microporous materials. The absence of significant hysteresis loops further confirms that monolayer adsorption within micropores was the dominant mechanism. As shown in Fig. 4b, the pore size distributions were predominantly concentrated in the micropore region below 2 nm, with an especially high fraction in the ultramicropore range (~0.5 nm), which aligns well with the molecular diameter of formaldehyde (~0.24 nm) [52]. Notably, AC-MB@KOH(3) showed the highest pore volume contribution in this optimal range. Structural parameters summarized in Table 1 reveal that increasing the A/C ratio from 1:1 to 4:1 led to a marked rise in the specific surface area (S_{BET}), ranging from 1526.75 to 2576.16 m^2/g, along with corresponding increases in total pore volume ($V_{0.99}$) and micropore volume (V_{micro}). Nevertheless, AC-MB@KOH(3) presented the best balance between surface area (2141.77 m^2/g) and a well-developed microporous network, providing abundant accessible adsorption sites and efficient molecular diffusion pathways. This structural synergy accounts for its superior adsorption performance. It is important to emphasize that surface area alone does not linearly determine adsorption efficiency. Despite AC-MB@KOH(4) exhibiting the highest S_{BET}, its formaldehyde adsorption performance was inferior to that of AC-MB@KOH(3). This suggests that optimal adsorption is governed not solely by total surface area, but by a synergistic interplay of factors, including pore size distribution, micropore accessibility, and the preservation of structural integrity. Overactivation can lead to the formation of non-selective or collapsed pores, which are less effective in adsorbing small, polar molecules like formaldehyde. In conclusion, KOH activation at a moderate A/C ratio (3:1) enables the formation of a highly microporous, structurally stable carbon framework. This optimizes the interaction between formaldehyde molecules and the carbon

surface, enhancing adsorption capacity and efficiency. These results highlight the potential of bamboo-based activated carbon as a sustainable and high-performance material for indoor VOC removal, particularly when activated via fine-tuned alkaline treatment.

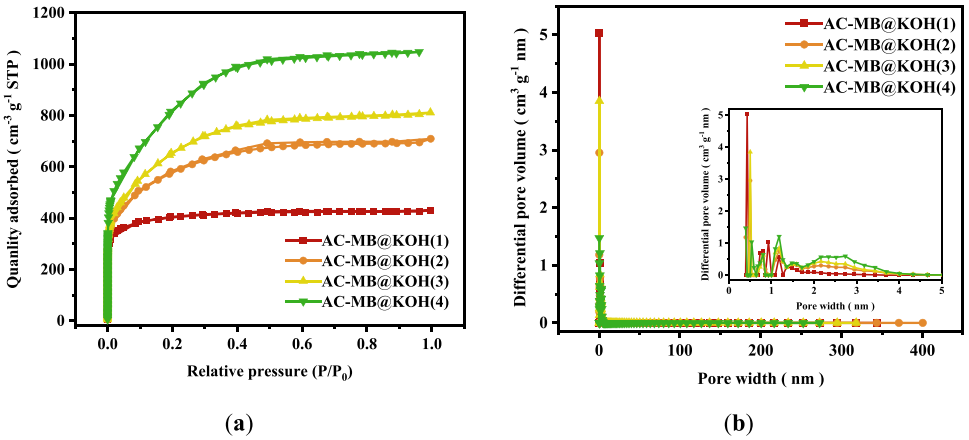

Figure 4: (**a**) N_2 adsorption/desorption isotherms and (**b**) pore size distribution curves of KOH-activated bamboo-derived carbon at various alkali-to-carbon ratios.

The mass yield of the activated carbon was calculated as the ratio of the final dried carbon mass to the initial mass of the dried bamboo precursor. Under the optimal activation condition (KOH, A/C = 3:1, 800°C), the yield of AC-MB@KOH(3) was approximately 17.6%, which falls within the typical yield range reported for strongly KOH-activated porous carbons [45]. The relatively reduced yield mainly originates from intensive chemical etching and gas evolution during activation, which promotes the formation of abundant micropores and large surface areas. In practical alkaline activation processes, potassium-containing species generated during activation can be partially recovered from the washing solution and potentially reused, thereby helping to mitigate the cost and environmental impact associated with strong chemical activation.

3.1.2 $KHCO_3$-Activated Bamboo-Based Carbon

To further assess the pore structure modulation capabilities of different alkaline activators, $KHCO_3$ was employed to activate bamboo-derived carbon. The formaldehyde adsorption performance of the resulting samples was systematically evaluated. As shown in Fig. 5, the adsorption capacity exhibited a non-linear trend with increasing alkali-to-carbon (A/C) ratios. The sample AC-MB@$KHCO_3$(2), prepared with an A/C ratio of 2:1, demonstrated the highest adsorption capacity of approximately 0.29 mg/g, corresponding to a formaldehyde removal efficiency of nearly 73%. Further increasing the A/C ratio to 3:1 or 4:1 did not lead to further improvement and instead resulted in a slight decline in performance. These results suggest that moderate activation facilitates pore development, while excessive $KHCO_3$ can compromise the structural integrity of the carbon matrix, thereby diminishing adsorption efficiency.

To elucidate the structural basis for these adsorption trends, nitrogen adsorption–desorption analyses were conducted. As depicted in Fig. 6a, all samples exhibited type-I isotherms, characteristic of microporous materials. A subtle hysteresis loop was observed at relative pressures $P/P_0 > 0.4$, indicating the presence of a minor fraction of mesopores. The corresponding pore size distributions in Fig. 6b confirmed that the dominant pore range lay between 0.5 and 2 nm, reinforcing the microporous nature of these carbons. However, unlike the KOH-activated counterparts, the $KHCO_3$-derived samples featured significantly lower pore structure metrics. As summarized in Table 2, the specific surface areas (S_{BET}) of $KHCO_3$-activated

samples ranged from 761.81 to 979.40 m^2/g, considerably lower than those of the KOH-activated samples. Similarly, the total pore volume ($V_{0.99}$) and micropore volume (V_{micro}) reached maximum values of 0.43 and 0.37 cm^3/g, respectively, for AC-MB@$KHCO_3$(2), but declined upon further increase in $KHCO_3$ dosage. These findings suggest that overactivation may cause partial pore collapse or degradation of the carbon framework, thereby diminishing accessible adsorption sites. Furthermore, the mesopore volume (V_{meso}) across all $KHCO_3$-activated samples remained extremely low, with AC-MB@$KHCO_3$(4) exhibiting a near-negligible value of 0.01 cm^3/g. This lack of mesoporosity implies poor molecular transport dynamics within the material, which may limit the enrichment of formaldehyde molecules near active adsorption regions.

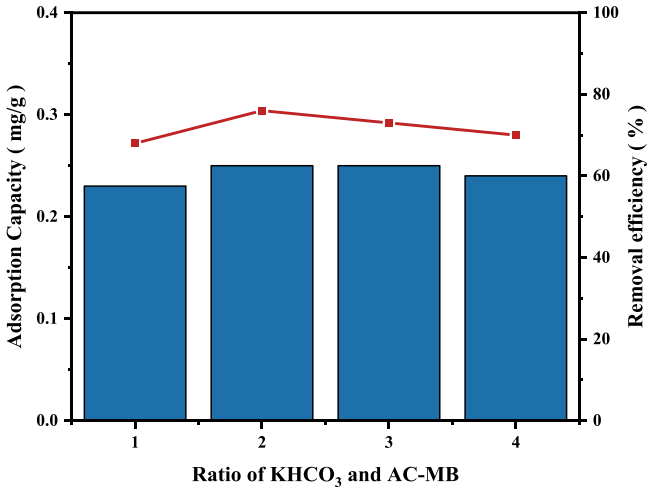

Figure 5: Formaldehyde adsorption performance of $KHCO_3$-activated bamboo-derived carbon with different alkali-to-carbon ratios.

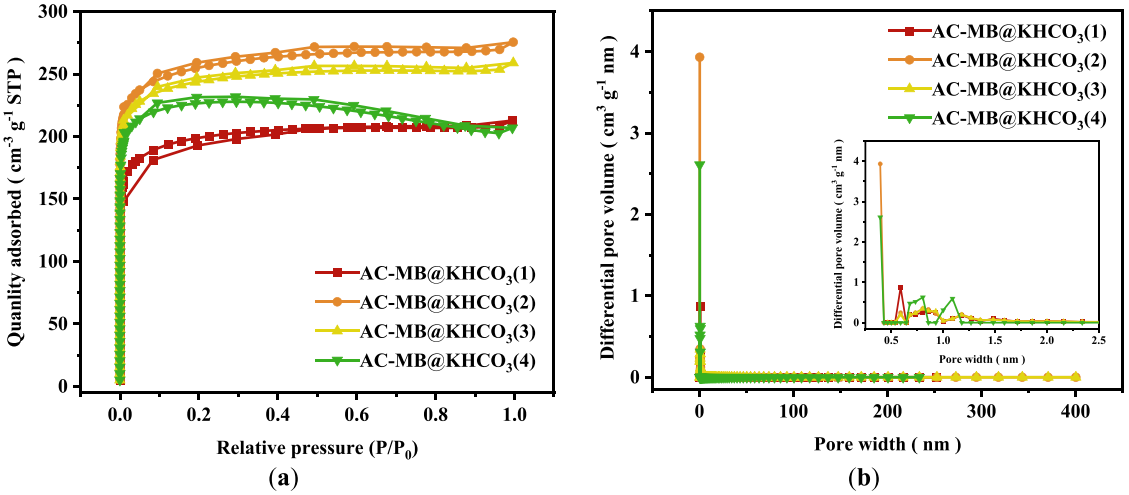

Figure 6: (**a**) N_2 adsorption/desorption isotherms and (**b**) pore size distribution curves of $KHCO_3$-activated bamboo-derived carbon at various alkali-to-carbon ratios.

Table 2: Pore structure parameters of $KHCO_3$-activated bamboo-derived carbon.

Sample	S_{BET} (m^2/g)	$V_{0.99}$ (cm^3/g)	V_{micro} (cm^3/g)	V_{meso} (cm^3/g)
AC-MB@$KHCO_3$(1)	761.81	0.33	0.29	0.04
AC-MB@$KHCO_3$(2)	979.40	0.43	0.37	0.05
AC-MB@$KHCO_3$(3)	941.33	0.40	0.36	0.04
AC-MB@$KHCO_3$(4)	882.96	0.35	0.34	0.01

Compared with KOH activation, $KHCO_3$ exhibits milder activation strength, resulting in significantly reduced surface area, pore volume, and hierarchical porosity. These structural limitations hinder the formation of a well-connected porous network required for efficient gas diffusion and capture. Moreover, the insufficient mesopore contribution may lead to increased mass transfer resistance, further limiting the material's adsorption capacity. Therefore, although $KHCO_3$ can moderately generate micropores under thermal treatment, its overall effectiveness in constructing high-performance adsorbents for formaldehyde removal is clearly inferior to that of KOH in this bamboo-derived carbon system.

3.1.3 K_2CO_3-Activated Bamboo-Based Carbon

To further explore the structural modulation effects of different alkaline activators on bamboo-derived carbon and their influence on formaldehyde adsorption, a series of samples were prepared using potassium carbonate (K_2CO_3) as the activating agent. As shown in Fig. 7, the formaldehyde adsorption capacity exhibited a typical "increase–decrease" trend with increasing alkali-to-carbon (A/C) ratios as above. Among them, the sample AC-MB@K_2CO_3(3), synthesized with an A/C ratio of 3:1, achieved the highest adsorption capacity of 0.27 mg/g, corresponding to a removal efficiency of approximately 81%, suggesting that this activation condition is optimal for formaldehyde purification.

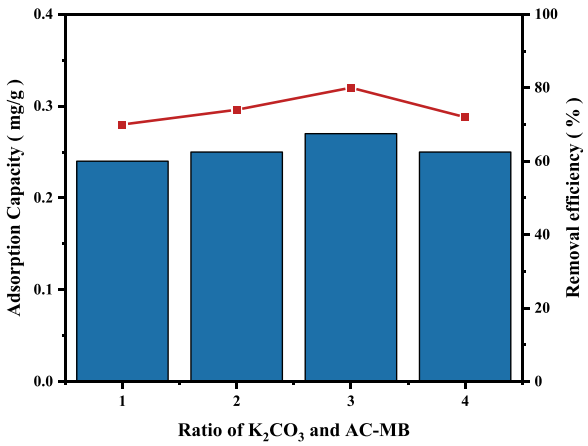

Figure 7: Formaldehyde adsorption performance of K_2CO_3-activated bamboo-derived carbon with different alkali-to-carbon ratios.

As illustrated in Fig. 8a, all K_2CO_3-activated samples displayed type I isotherms, characteristic of microporous materials. A slight hysteresis loop was observed at relative pressures $P/P_0 > 0.4$, indicating the coexistence of mesoporous features within the structure. The corresponding pore size distributions in Fig. 8b revealed that most pores were concentrated in the 0.5–2 nm range, with ultramicropores (~0.5 nm) being dominant, which is highly favorable for adsorbing small molecules such as formaldehyde (molecular

diameter ~0.24 nm). As summarized in Table 3, the specific surface area (S_{BET}) of the samples initially increased from 1065.45 m^2/g to a peak value of 1404.17 m^2/g as the A/C ratio increased, followed by a slight decline at higher dosages. Notably, AC-MB@K_2CO_3(3) also exhibited the highest total pore volume (0.67 cm^3/g) and micropore volume (0.52 cm^3/g), confirming that a moderate K_2CO_3 content can effectively promote the development of a micropore-rich network with adequate adsorption sites. In addition, the mesopore volume (Vmeso) of K_2CO_3-activated samples ranged from 0.07 to 0.17 cm^3/g, slightly higher than that of the $KHCO_3$ group. This suggests a more developed hierarchical pore structure, which benefits the diffusion and transport of gas molecules throughout the carbon matrix.

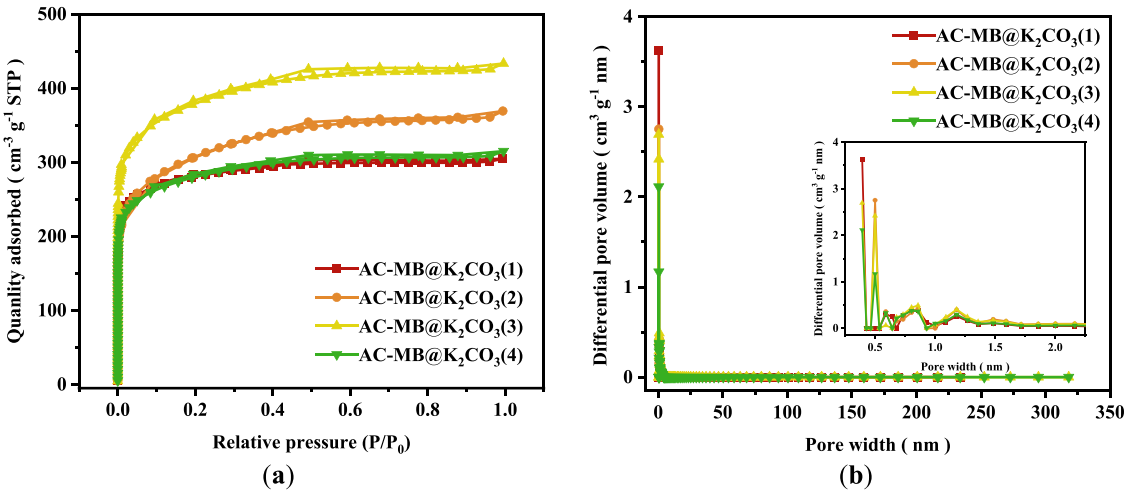

Figure 8: (**a**) N_2 adsorption/desorption isotherms and (**b**) pore size distribution curves of K_2CO_3-activated bamboo-derived carbon at various alkali-to-carbon ratios.

Table 3: Pore structure parameters of K_2CO_3-activated bamboo-derived carbon.

Sample	S_{BET} (m^2/g)	$V_{0.99}$ (cm^3/g)	V_{micro} (cm^3/g)	V_{meso} (cm^3/g)
AC-MB@K_2CO_3(1)	1065.45	0.47	0.40	0.07
AC-MB@K_2CO_3(2)	1107.64	0.57	0.40	0.17
AC-MB@K_2CO_3(3)	1404.17	0.67	0.52	0.15
AC-MB@K_2CO_3(4)	1043.47	0.49	0.39	0.09

Importantly, the activation strength of K_2CO_3 lies between that of KOH and $KHCO_3$. It offers sufficient pore-etching capability while better maintaining the structural integrity of the carbon framework compared to the more aggressive KOH treatment. However, further increasing the A/C ratio to 4:1 resulted in a decline in adsorption performance, potentially due to partial sintering or the collapse of internal pores, leading to a reduction in effective adsorption sites. These findings indicate that maintaining a balanced activation level is crucial, since overactivation may compromise structural stability, while underactivation may fail to generate the necessary porosity. Thus, the K_2CO_3 activation system demonstrates the importance of synergistically tuning pore structure and material robustness to optimize the adsorption properties of bamboo-based carbon adsorbents.

3.2 Structure and Performance Relationship Analysis

To elucidate the intrinsic relationship between the structural features of bamboo-derived activated carbons and their formaldehyde removal performance, correlation analyses were conducted between removal efficiency and key pore structure parameters, as shown in Fig. 9. The results show that the formaldehyde removal rate exhibits a strong linear relationship with specific surface area (R^2 = 0.88), indicating that larger accessible surface areas contribute significantly to enhancing adsorption. Similarly, a notable correlation was found with total pore volume (R^2 = 0.83), suggesting that increased internal porosity facilitates molecular diffusion and retention. More importantly, micropore volume demonstrated a high degree of correlation (R^2 = 0.87), underscoring its dominant role in trapping formaldehyde molecules. Considering the kinetic diameter of formaldehyde (~0.24 nm), the sub-nanometer pores generated during activation act as effective molecular sieves that selectively capture formaldehyde gas. In contrast, mesopore volume exhibited a slightly weaker correlation (R^2 = 0.76), indicating that while mesopores aid in gas transport and structural buffering, they play a secondary role in direct adsorption.

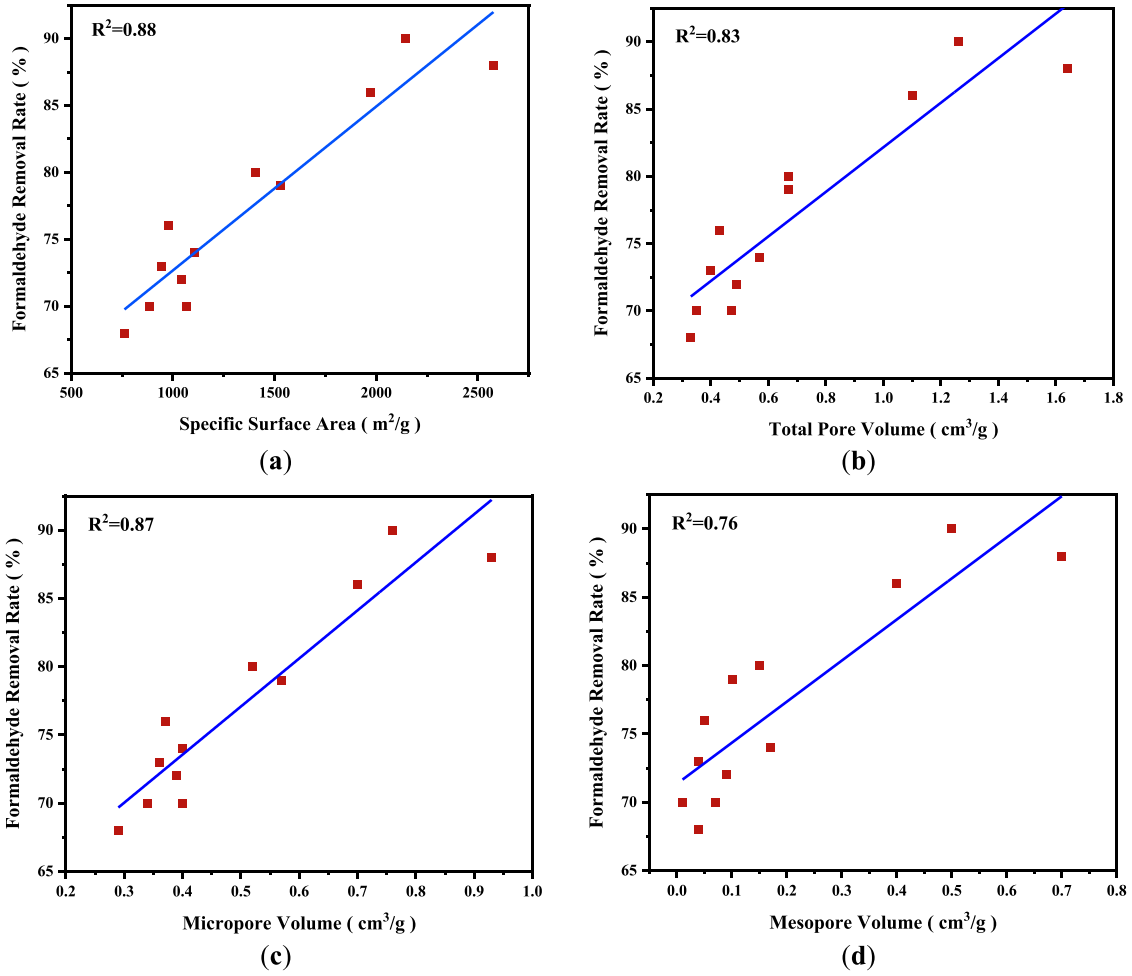

Figure 9: Correlations between formaldehyde removal efficiency and (**a**) specific surface area (S_{BET}), (**b**) total pore volume ($V_{0.99}$), (**c**) micropore volume (V_{micro}), and (**d**) mesopore volume (V_{meso}).

Integrating the correlation data from Fig. 9 with the pore characteristics summarized in Tables 1–3, it is evident that KOH activation most effectively constructs hierarchical porous networks rich

in accessible micropores. Compared with $KHCO_3$ and K_2CO_3, the strong etching and gas-evolving nature of KOH promotes the formation of narrowly distributed micropores, which are well-suited to the molecular size of formaldehyde. This optimized pore architecture results in superior adsorption performance. Overall, the formaldehyde adsorption capacity of bamboo-derived activated carbons is fundamentally governed by micropore content and total porosity. A high-density microporous structure provides sufficient active sites, while the mesoporous framework ensures rapid transport and diffusion of formaldehyde gas molecules [53,54]. These findings highlight KOH as an efficient activating agent for designing advanced porous adsorbents for indoor air purification and building-related environmental remediation.

3.3 Comparative Evaluation of Bamboo-Based Carbons Modified by Different Activating Agents

To comprehensively evaluate the influence of different alkaline activating agents on the pore structure and adsorption performance of bamboo-derived activated carbons, three representative activators-KOH, $KHCO_3$, and K_2CO_3-were employed under a fixed alkali-to-carbon ratio of 3:1 for cross-agent comparison. The structural parameters and adsorption results are summarized in Table 4. Among the three samples, AC-MB@KOH(3) exhibited the most outstanding performance, delivering a specific surface area of 2141.77 m^2/g, a formaldehyde adsorption capacity of 0.34 mg/g, and a removal efficiency of 90%. These values are significantly higher than those obtained for AC-MB@$KHCO_3$(3) (0.25 mg/g, 73%) and AC-MB@K_2CO_3(3) (0.27 mg/g, 81%). The results clearly demonstrate that the choice of activating agent plays a decisive role in regulating pore development and adsorption performance. Under identical precursor and activation conditions, KOH at A/C = 3:1 provides the most effective pore-structure engineering route among the three potassium-based activators evaluated in this work. Similar trends have been reported in previous studies on chemically activated carbons, where stronger activating agents typically induce more intensive carbon etching and promote the formation of highly developed microporous structures [9,45,55,56]. It should be noted that adsorption capacities reported in different studies may vary significantly due to differences in experimental conditions such as initial concentration, humidity, and evaluation methods. Therefore, direct quantitative comparison of adsorption capacities across different studies is not always appropriate. Nevertheless, the present results remain consistent with the widely reported trend that stronger alkaline activation favors the development of microporous structures and enhances gas-phase adsorption performance [20,25].

Table 4: Comparison of structure and performance of bamboo-derived carbon activated by different alkalis.

Sample	SBET (m^2/g)	Adsorption Capacity (mg/g)	Removal Efficiency (%)
AC-MB@KOH(3)	2141.77	0.34	90
AC-MB@KHCO3(3)	941.33	0.25	73
AC-MB@K2CO3(3)	1404.17	0.27	81

To further evaluate the adsorption kinetics of the three activated carbons under identical conditions, the time-dependent formaldehyde removal efficiencies are presented in Fig. 10. All samples exhibit a rapid increase in removal efficiency during the initial stage, followed by a gradual approach toward equilibrium. The fast initial adsorption stage can be attributed to the large number of accessible adsorption sites and rapid diffusion of formaldehyde molecules into the porous network. Among the three materials, AC-MB@KOH(3) shows the fastest adsorption rate and the highest equilibrium removal efficiency (~90%), whereas AC-MB@K_2CO_3(3) and AC-MB@$KHCO_3$(3) exhibit slower adsorption kinetics and lower final efficiencies. This trend is consistent with the pore structure characteristics summarized in Table 4, indicating that the

enhanced micropore development induced by strong KOH activation significantly improves both adsorption capacity and adsorption kinetics for gas-phase formaldehyde capture.

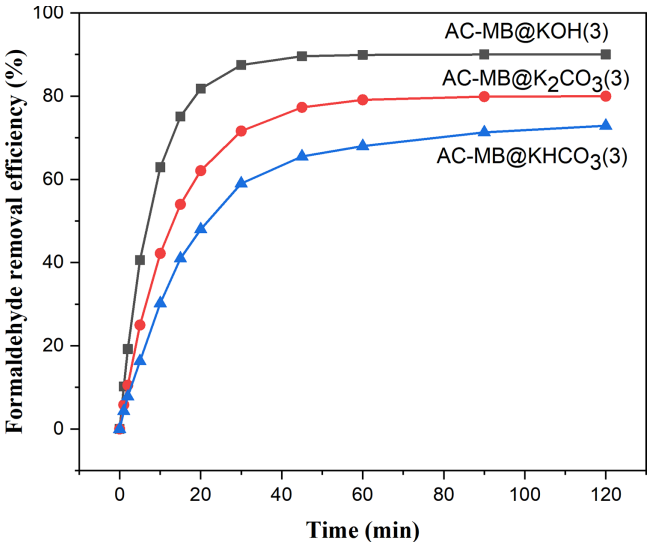

Figure 10: Time-dependent formaldehyde removal efficiencies of AC-MB@$KHCO_3$(3), AC-MB@K_2CO_3(3), and AC-MB@KOH(3).

The superior performance of the KOH-activated carbon can be further understood from the perspective of activation chemistry. As a strong alkaline activator, KOH reacts vigorously with carbon at elevated temperatures, generating potassium-containing intermediates and gaseous species such as H_2, CO, and CO_2. The *in situ* release and diffusion of these gases within the carbon framework create a pore formation effect that promotes extensive carbon etching and pore expansion, resulting in the formation of abundant micropores and interconnected porous networks. In contrast, $KHCO_3$ and K_2CO_3 exhibit milder activation behavior. $KHCO_3$ first decomposes into K_2CO_3 during heating and then participates in subsequent activation reactions, while the gas release during this process is relatively slow and insufficient to induce intensive pore development. K_2CO_3 activation typically requires higher temperatures to initiate effective carbon etching and may cause localized sintering or partial structural collapse at excessive loadings.

Beyond the activation chemistry, the enhanced formaldehyde removal performance can also be attributed to the adsorption mechanism associated with the developed pore structure and surface chemistry. Micropores in the range of approximately 0.5–2 nm provide a size-matching confinement environment for small formaldehyde molecules (kinetic diameter ≈ 0.24 nm), enabling efficient adsorption through van der Waals interactions and pore-filling effects [57]. Meanwhile, oxygen- and nitrogen-containing functional groups on the carbon surface can enhance surface polarity, thereby strengthening dipole–dipole interactions and weak chemisorption with formaldehyde molecules. Furthermore, the coexistence of micropores and mesopores forms a hierarchical pore architecture that facilitates rapid gas diffusion and improves accessibility to internal adsorption sites. This synergistic combination of micropore adsorption, surface polarity, and improved mass transport ultimately results in the superior adsorption performance observed for AC-MB@KOH(3).

To further verify the structural characteristics responsible for the superior adsorption performance, AC-MB@KOH(3) was selected for scanning electron microscopy (SEM) and energy-dispersive X-ray spectroscopy (EDS) analysis. As shown in Fig. 11, the low-magnification SEM image (Fig. 11a) reveals that the activated carbon largely preserves the macroscopic morphology of the bamboo precursor, with

visible grooves and surface textures. The high-magnification image (Fig. 11b) clearly displays numerous uniformly distributed pores, suggesting that the strong etching effect induced by high-temperature KOH activation effectively facilitates pore formation and surface roughening. In addition, the EDS elemental mapping (Fig. 11c) confirms that the carbon framework is primarily composed of C, with minor amounts of O and N uniformly distributed on the surface. These heteroatoms likely originate from the intrinsic composition of bamboo and residual functional groups generated during carbonization and activation, which may contribute to additional physical adsorption or weak chemical interactions with formaldehyde molecules [58].

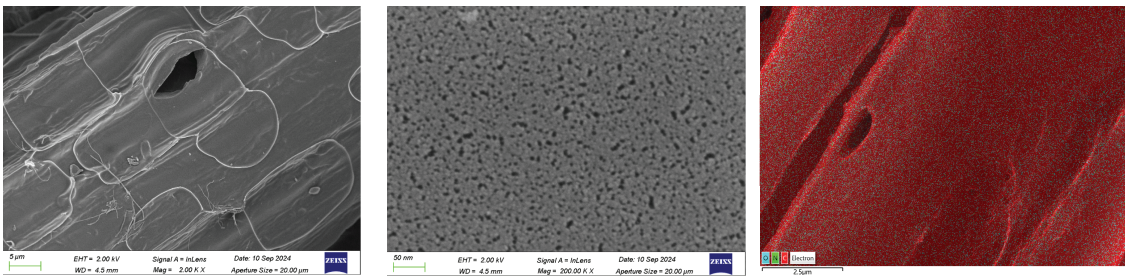

(a) (b) (c)

Figure 11: (**a**,**b**) SEM images and (**c**) EDS mapping of AC-MB@KOH(3).

In practical indoor environments, formaldehyde often coexists with moisture and other VOC molecules, which may introduce competitive adsorption effects. In particular, water vapor may partially occupy adsorption sites or influence molecular diffusion within micropores under humid conditions. Nevertheless, the well-developed microporous structure of the present bamboo-derived carbons is expected to maintain effective adsorption of small formaldehyde molecules. From an application perspective, regeneration and post-use handling of the adsorbent are also important considerations for sustainable utilization. Adsorbed formaldehyde can potentially be removed through thermal or vacuum-assisted desorption processes, allowing the adsorbent to be reused. Moreover, bamboo-derived carbons exhibit good thermal stability and may be further regenerated by mild heat treatment or repurposed for other carbon-based applications. These characteristics indicate that the present bamboo-based adsorbents are compatible with sustainable material utilization strategies and practical indoor air purification applications.

4 Conclusion

In this study, a series of bamboo-derived activated carbons were synthesized using three alkaline activating agents-KOH, $KHCO_3$, and K_2CO_3-to investigate their structure–performance relationships in formaldehyde adsorption. Among the three, the KOH-activated sample exhibited the most outstanding performance, achieving the highest specific surface area (2141.77 m^2/g), a formaldehyde uptake capacity of 0.34 mg/g, and a removal efficiency of 90%. This superior adsorption behavior is attributed to KOH's strong activation strength and abundant gas evolution during thermal treatment, which collectively promoted the formation of a highly microporous and hierarchically porous architecture. Correlation analysis revealed that micropore volume played the most critical role in determining adsorption efficiency, highlighting the importance of size-matching between micropores and formaldehyde molecules. Compared with $KHCO_3$ and K_2CO_3, KOH demonstrated superior capability in tailoring pore structure and enhancing adsorption performance. Overall, this work provides a feasible and scalable strategy for producing high-efficiency, biomass-derived porous adsorbents through rational activation design. These results provide practical guidance for developing cost-effective, environmentally friendly adsorbents for indoor air quality improvement.

Acknowledgement: This work was supported by the Zhenghe Rural Revitalization Research Institute of Fujian Agriculture and Forestry University.

Funding Statement: We gratefully acknowledge the support of the central government guides local funds for scientific and technological development (Grant No. 2023L3044), the Natural Science Foundation of Fujian Province, China (Grant No. 2023J01462), the Fujian Provincial Science and Technology Project (Industry-University Cooperation Project for Higher Education Institutions, Grant No. 2025H6008) and the Fujian Provincial Science and Technology Project (Technological Innovation Project, Grant No. 2024C0019), Fujian Agriculture and Forestry University Science and Technology innovation special fund project (Grant Nos. KFB23142, KFB24010).

Author Contributions: The authors confirm contribution to the paper as follows: Conceptualization, Weigang Zhao and Ju He; methodology, Ju He and Peiwen Zhao; software, Ju He; validation, Ju He, Dongyang Han and Kexin Lv; formal analysis, Ju He and Peiwen Zhao; investigation, Ju He, Peiwen Zhao and Dongyang Han; resources, Weigang Zhao, Xinqiang Ye, Guodong Ruan, Fei Guo, Mizi Fan and Jiuping Rao; data curation, Ju He; writing—original draft preparation, Ju He; writing-review and editing, Weigang Zhao and Ju He; visualization, Ju He; supervision, Weigang Zhao; project administration, Weigang Zhao; funding acquisition, Weigang Zhao. All authors reviewed and approved the final version of the manuscript.

Availability of Data and Materials: Data available on request from the authors.

Ethics Approval: Not applicable.

Conflicts of Interest: The authors declare no conflicts of interest.

References

1. Dimitroulopoulou S, Dudzińska MR, Gunnarsen L, Hägerhed L, Maula H, Singh R, et al. Indoor air quality guidelines from across the world: an appraisal considering energy saving, health, productivity, and comfort. Environ Int. 2023;178(11):108127. doi:10.1016/j.envint.2023.108127.
2. Rasheed H, Jayasree TK. The multifaceted role of indoor plants: a comprehensive review of their impact on air quality, health, and perception. Energy Build. 2025;330:115312. doi:10.1016/j.enbuild.2025.115312.
3. Yang S, Mahecha SD, Moreno SA, Licina D. Integration of indoor air quality prediction into healthy building design. Sustainability. 2022;14(13):7890. doi:10.3390/su14137890.
4. Bie S, Nie S. The effect of water co-adsorption on the adsorption of formaldehyde in Fe-HHTP-MOF metal-organic materials. ACS Omega. 2024;9(51):50300–7. doi:10.1021/acsomega.4c06322.
5. Sun Z, Wang Z, Yang X, An K, Qu Z, Tang Z, et al. Synergistic mechanism of formaldehyde adsorption by intrinsic defects and carboxyl groups on the surface of carbon materials. Chemosphere. 2023;337:139351. doi:10.1016/j.chemosphere.2023.139351.
6. Zhang Y, Xu N, Liu J, Guo Z, Guan H, Bai Y. A multisource mass transfer model for simulating VOC emissions from paints. Sci Total Environ. 2023;902(1):165945. doi:10.1016/j.scitotenv.2023.165945.
7. Richter M, Horn W, Juritsch E, Klinge A, Radeljic L, Jann O. Natural building materials for interior fitting and refurbishment-what about indoor emissions? Materials. 2021;14(1):234. doi:10.3390/ma14010234.
8. Kang YJ, Jo HK, Jang MH, Ma X, Jeon Y, Oh K, et al. A brief review of formaldehyde removal through activated carbon adsorption. Appl Sci. 2022;12(10):5025. doi:10.3390/app12105025.
9. Lara-Ibeas I, Megías-Sayago C, Louis B, Le CS. Adsorptive removal of gaseous formaldehyde at realistic concentrations. J Environ Chem Eng. 2020;8(4):103986. doi:10.1016/j.jece.2020.103986.
10. Jung C, Abdelaziz Mahmoud NS. Ventilation strategies for mitigating indoor air pollutants in high-rise residential buildings: a case study in Dubai. Atmosphere. 2023;14(11):1600. doi:10.3390/atmos14111600.
11. Ren B, Wu Q, Muskhelishvili L, Davis K, Wang Y, Rua D, et al. Evaluating the sub-acute toxicity of formaldehyde fumes in an *in vitro* human airway epithelial tissue model. Int J Mol Sci. 2022;23(5):2593. doi:10.3390/ijms23052593.

12. Song J, Liu Z, Li Y, Chi C, Zhang Y, Jiang G. Preparation of amino cellulose aerogel and its formaldehyde adsorption properties. Ind Crops Prod. 2024;215:118630. doi:10.1016/j.indcrop.2024.118630.
13. Schumacher S, Caspari A, Schneiderwind U, Staack K, Sager U, Asbach C. The drawback of optimizing air cleaner filters for the adsorption of formaldehyde. Atmosphere. 2024;15(1):109. doi:10.3390/atmos15010109.
14. Su C, Liu K, Guo J, Ma W, Li H, Zeng Z, et al. Development of nitrogen-enriched carbon materials by the subtraction method for formaldehyde adsorption. Surf Interfaces. 2021;24(20):101038. doi:10.1016/j.surfin.2021.101038.
15. Becker A, Israfilov N, Ehrstein E, Lara-Ibeas I, Planeix JM, Louis B, et al. Adsorption of gaseous formaldehyde on Y zeolites and on metal-organic frameworks. Microporous Mesoporous Mater. 2022;343:112136. doi:10.1016/j.micromeso.2022.112136.
16. Park S, Lee JI, Na CK, Kim D, Kim JJ, Kim DY. Evaluation of the adsorption performance and thermal treatment-associated regeneration of adsorbents for formaldehyde removal. J Air Waste Manag Assoc. 2024;74(2):131–44. doi:10.1080/10962247.2023.2292205.
17. Dong X, Song C, Li L, Si W, Cao J, Liu F, et al. Surface curvature modulation of the boron nitride nanocage to boost formaldehyde adsorption and catalytic oxidation. Mol Catal. 2024;553:113757. doi:10.1016/j.mcat.2023.113757.
18. Jhang SR, Chou FC, Huang YC, Chen SC, Lin YC. Formaldehyde adsorption by amine-modified functional group over zeolite based nano-photocatalyst. Inorg Chem Commun. 2024;170:113343. doi:10.1016/j.inoche.2024.113343.
19. An K, Wang Z, Yang X, Qu Z, Sun F, Zhou W, et al. Reasons of low formaldehyde adsorption capacity on activated carbon: multi-scale simulation of dynamic interaction between pore size and functional groups. J Environ Chem Eng. 2022;10(6):108723. doi:10.1016/j.jece.2022.108723.
20. Law CK, Lai JHK, Ma XD, Sze-To GN. Enhancing indoor air quality: examination of formaldehyde adsorption efficiency of portable air cleaner fitted with chemically-treated activated carbon filters. Build Environ. 2024;263(3):111823. doi:10.1016/j.buildenv.2024.111823.
21. Shao S, Kim HW, Kim SS, Chen Y, Lai M. NGQDs modified nanoporous TiO_2/graphene foam nanocomposite for excellent sensing response to formaldehyde at high relative humidity. Appl Surf Sci. 2020;516:145932. doi:10.1016/j.apsusc.2020.145932.
22. Chen Z, Chen Q, Wang Y, Zou W, Li Y, Mo J. Tuning multi-scale pore structures in carbonaceous films via direct ink writing and sacrificial templates for efficient indoor formaldehyde removal. J Hazard Mater. 2025;487(4):137203. doi:10.1016/j.jhazmat.2025.137203.
23. Chen T, Hu X, Zhao T, Ge Y. Nitrogen and oxygen Co-doped porous carbon fabric for efficient removal of formaldehyde. Fibres Polym. 2022;23(7):1888–93. doi:10.1007/s12221-022-4143-y.
24. Chang SM, Hu SC, Shiue A, Lee PY, Leggett G. Adsorption of silver nano-particles modified activated carbon filter media for indoor formaldehyde removal. Chem Phys Lett. 2020;757(4):137864. doi:10.1016/j.cplett.2020.137864.
25. Jiao Y, Wang Z, Zhao H, Meng E, Sun Z, Yang L, et al. Effect of nitrogen-doped activated carbon on formaldehyde adsorption behaviour in different scale pores. Appl Surf Sci. 2024;670:160686. doi:10.1016/j.apsusc.2024.160686.
26. Li X, Zhang L, Yang Z, Wang P, Yan Y, Ran J. Adsorption materials for volatile organic compounds (VOCs) and the key factors for VOCs adsorption process: a review. Sep Purif Technol. 2020;235:116213. doi:10.1016/j.seppur.2019.116213.
27. Zhao H, An K, Wang Z, Liu X, He M, Yang X, et al. The impact of water co-adsorption on the removal of formaldehyde from the indoor air by oxygen-rich activated carbons: a theoretical and experimental study. Appl Surf Sci. 2023;635:157729. doi:10.1016/j.apsusc.2023.157729.
28. Zhao R, Liu G, Wei G, Gao J, Lu H. Analysis of SO(2) physisorption by edge-functionalized nanoporous carbons using grand canonical Monte Carlo methods and density functional theory: implications for SO(2) removal. ACS Omega. 2021;6(49):33735–46. doi:10.1021/acsomega.1c05000.
29. Canevesi RLS, Schaefer S, Izquierdo MT, Celzard A, Fierro V. Roles of surface chemistry and texture of nanoporous activated carbons in CO_2 capture. ACS Appl Nano Mater. 2022;5(3):3843–54. doi:10.1021/acsanm.1c04474.
30. Hong Y, Jin HJ, Kwak HW. Nitrogen-rich magnetic bio-activated carbon from sericin: a fast removable and easily separable superadsorbent for anionic dye removal. Macromol Res. 2020;28(11):986–96. doi:10.1007/s13233-020-8132-y.

31. Guo X, Zhang G, Wu C, Liu J, Li G, Zhao Y, et al. A cost-effective synthesis of heteroatom-doped porous carbon by sulfur-containing waste liquid treatment: as a promising adsorbent for CO_2 capture. J Environ Chem Eng. 2021;9(2):105165. doi:10.1016/j.jece.2021.105165.
32. Yu H, Mikšík F, Thu K, Miyazaki T. Characterization and optimization of pore structure and water adsorption capacity in pinecone-derived activated carbon by steam activation. Powder Technol. 2024;431(4):119084. doi:10.1016/j.powtec.2023.119084.
33. Zhao X, Zheng B, Xia H, Su Y, Wang H, Hu E, et al. Effective removal of beryllium from industrial wastewater by alkali-leaching activated carbon. Water Air Soil Pollut. 2023;234(9):568. doi:10.1007/s11270-023-06577-1.
34. Fu H, Zhang J, Zhao L, Huang Y, Chen B. Investigations of NO reduction by coal-based activated carbon with KOH activation: performance and mechanism. Chemosphere. 2024;346:140506. doi:10.1016/j.chemosphere.2023.140506.
35. Xu Y, Liu Y, Zhan W, Zhang D, Liu Y, Xu Y, et al. Enhancing CO_2 capture with K_2CO_3-activated carbon derived from peanut shell. Biomass Bioenergy. 2024;183(13):107148. doi:10.1016/j.biombioe.2024.107148.
36. Wu C, Liu J, Wang Y, Zhao Y, Li G, Zhang Y, et al. A clean method for controlling pore structure development in potassium activation systems to improve CO_2 adsorption properties of biochar. Sci Total Environ. 2024;954:176429. doi:10.1016/j.scitotenv.2024.176429.
37. Baran P, Buczek B, Zarębska K. Modified activated carbon as an effective hydrogen adsorbent. Energies. 2022;15(17):6122. doi:10.3390/en15176122.
38. Rehman A, Heo YJ, Nazir G, Park SJ. Solvent-free, one-pot synthesis of nitrogen-tailored alkali-activated microporous carbons with an efficient CO_2 adsorption. Carbon N Y. 2021;172:71–82. doi:10.1016/j.carbon.2020.09.088.
39. Khuong DA, Trinh KT, Nakaoka Y, Tsubota T, Tashima D, Nguyen HN, et al. The investigation of activated carbon by K(2)CO(3) activation: micropores- and macropores-dominated structure. Chemosphere. 2022;299:134365. doi:10.1016/j.chemosphere.2022.134365.
40. Kim JH, Lee G, Park JE, Kim SH. Limitation of K_2CO_3 as a chemical agent for upgrading activated carbon. Processes. 2021;9(6):1000. doi:10.3390/pr9061000.
41. Peng B, Zhu Y, Chu S, Zhang H. N-doped hierarchical porous carbons derived from heavy bio-oil for supercapacitor applications. Chem Eng J. 2025;507(8):160551. doi:10.1016/j.cej.2025.160551.
42. Dou Z, Chen H, Liu Y, Huang R, Pan J. Removal of gaseous H_2S using microalgae porous carbons synthesized by thermal/microwave KOH activation. J Energy Inst. 2022;101(3):45–55. doi:10.1016/j.joei.2021.12.007.
43. Huang Y, Hu J, Zhang Y, Yu Y, Zhang D, Jing Q, et al. Multifunctional bamboo based materials empowered by multiscale hierarchical structures-a critical review. Adv Mater. 2026;38(2):e07844. doi:10.1002/adma.202507844.
44. Gao Q, Gan J, Wang P, Huang Y, Zhang D, Yu W. Bio-inspired hierarchical bamboo-based air filters for efficient removal of particulate matter and toxic gases. Exploration. 2024;5(1):20240012. doi:10.1002/EXP.20240012.
45. Zhao W, Luo L, Chen T, Li Z, Zhang Z, Wang H, et al. Synthesis and characterization of Pt-N-doped activated biocarbon composites for hydrogen storage. Compos Part B Eng. 2019;161(7):464–72. doi:10.1016/j.compositesb.2018.12.122.
46. Chen Y, Yin H, Wen S, Zhang W, Hu S, Sun K, et al. Biogas upgrading using aqueous bamboo-derived activated carbons. Bioresour Technol. 2025;419(3):132055. doi:10.1016/j.biortech.2025.132055.
47. Chaudhuri P, Pande R, Baraiya NA. From char to flame: evaluating bamboo bio-char combustion via cone calorimetry and thermogravimetric analysis. Energy. 2025;314:134313. doi:10.1016/j.energy.2024.134313.
48. Vali IP, Anusha BS, Pruthvija M, Savitha S, Ravindra S, Nagaveni M, et al. Bamboo and coconut shell based activated carbon: a Raman spectroscopic study. Mater Chem Phys. 2024;318:129240. doi:10.1016/j.matchemphys.2024.129240.
49. Chaturvedi K, Singhwane A, Dhangar M, Mili M, Gorhae N, Naik A, et al. Bamboo for producing charcoal and biochar for versatile applications. Biomass Convers Biorefin. 2023:1–27. doi:10.1007/s13399-022-03715-3.
50. Liu H, Xu C, Wei X, Ren Y, Tang D, Zhang C, et al. 3D hierarchical porous activated carbon derived from bamboo and its application for textile dye removal: kinetics, isotherms, and thermodynamic studies. Water Air Soil Pollut. 2020;231(10):504. doi:10.1007/s11270-020-04883-6.

51. Alfatah T, Mistar EM, Supardan MD. Porous structure and adsorptive properties of activated carbon derived from *Bambusa vulgaris Striata* by two-stage KOH/NaOH mixture activation for Hg^{2+} removal. J Water Process Eng. 2021;43:102294. doi:10.1016/j.jwpe.2021.102294.
52. Wei H, Deng S, Hu B, Chen Z, Wang B, Huang J, et al. Granular bamboo-derived activated carbon for high CO_2 adsorption: the dominant role of narrow micropores. ChemSusChem. 2012;5(12):2354–60. doi:10.1002/cssc.201200570.
53. Zhang Y, Zhang Z, Zheng J, Peng R, Chang M, Hu F, et al. Sequential double chemical activation of biochar enables the fast and high-capacity capture of tetracycline. Mater Chem Front. 2024;8(19):3242–56. doi:10.1039/d4qm00381k.
54. He D, Wu J, Yu C, Huang B, Tu X, Li D, et al. Synthesis of corncob biochar with high surface area by KOH activation for VOC adsorption: effect of KOH addition method. J Chem Technol Biotechnol. 2023;98(8):2051–64. doi:10.1002/jctb.7418.
55. Lillo-Ródenas MA, Cazorla-Amorós D, Linares-Solano A. Understanding chemical reactions between carbons and NaOH and KOH An insight into the chemical activation mechanism. Carbon. 2003;41(2):267–75. doi:10.1016/S0008-6223(02)00279-8.
56. Luo L, Luo L, Deng J, Chen T, Du G, Fan M, et al. High performance supercapacitor electrodes based on B/N Co-doped biomass porous carbon materials by KOH activation and hydrothermal treatment. Int J Hydrogen Energy. 2021;46(63):31927–37. doi:10.1016/j.ijhydene.2021.06.211.
57. Zhao H, Tang Z, He M, Yang X, Lai S, An K, et al. Effect of oxygen functional groups on competitive adsorption of benzene and water on carbon materials: density functional theory study. Sci Total Environ. 2023;863(6):160772. doi:10.1016/j.scitotenv.2022.160772.
58. Kowalska K, Barczak M, Giannakoudakis DA, Bandosz TJ, Borowski P. Formaldehyde interactions with oxygen- and nitrogen-functionalized carbonaceous surfaces in the presence of moisture: computational approach vs. experimental results. Carbon N Y. 2023;215:118443. doi:10.1016/j.carbon.2023.118443.